Separation and Purification Technology 287 (2022) 120557

Contents lists available at ScienceDirect

Separation and Purification Technology

journal homepage: www.elsevier.com/locate/seppur

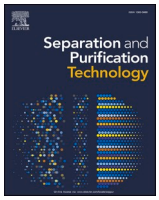

Simulation of SO_2 removal process from marine exhaust gas by hybrid exhaust gas cleaning systems (EGCS) using seawater and magnesium-based absorbent

Zhongyang Zhao [a], Yongxin Zhang [a], Yuhao Shao [a], Chang Liu [a], Wenjun Li [a], Haidong Fan [a], Haobo Dai [b], Yang Yang [a,*], Chenghang Zheng [a,c,*], Xiang Gao [a,c]

[a] State Key Laboratory of Clean Energy Utilization, State Environmental Protection Center for Coal-Fired Air Pollution Control, Zhejiang University, Hangzhou 310027, China
[b] Zhejiang Tiandi Environmental Protection Engineering Co., Ltd, Hangzhou 310012, China
[c] Ningbo Research Institute, Zhejiang University, Ningbo 315100, China

ARTICLE INFO

Keywords:
SO_2 absorption
Exhaust gas cleaning system
Seawater
Magnesium-based absorbent
Operation strategy

ABSTRACT

Exhaust gas from navigation is an important source of air pollution, especially in coastal and port cities. The installation of a hybrid exhaust gas cleaning system (EGCS) is a popular method to reduce the SO_2 emission because of their flexibility and efficiency. However, limited by the experience of operators, the operation of EGCS can hardly meet the requirement of economy and safety demands. In this paper, a detailed model of hybrid EGCS is developed to study the effect of important factors on SO_2 absorption process and crystallization process. A comparison between seawater and magnesium-based absorbent on the SO_2 absorption process in the droplet and the scrubber is carried out. Compared with seawater, magnesium-based absorbents are more adaptable to temperature and the SO_2 concentration. What's more, in order to prevent the EGCS from scaling and ensure the safe operation of EGCS, the safe operating ranges of magnesium-based absorbent under different temperature and oxidation rate are studied. Finally, an operation strategy of the EGCS for different absorbents is proposed. The operator can adjust the liquid-gas ratio of the current operating mode or switch to other modes according to the temperature and pH of seawater and emission standard. These results would be helpful for the design and the operation of the EGCS.

1. Introduction

The combustion of fossil fuels such as coal, oil and gas are the main sources of SO_2 emissions[1]. And, exhaust gas from navigation is an important source of SO_2 pollution[2] (about 13% of global SO_x annual emissions), especially in coastal and port cities. For example, in 2019, the SO_2 emission from domestic navigation account for 7% of total SO_x emission in U.K.[3]. According to *2018 Hong Kong Emission Inventory Report*, in 2018, SO_2 emissions from navigation accounted for 49% of total SO_2 emissions in Hong Kong[4]. Recently, people have paid more attention to SO_2 pollution due to its adverse effects on human health[5] and air quality[6,7]. In order to reduce the emission of pollutants from navigation, the 58th meeting of the Marine Environmental Protection Committee (MEPC) passed the amendment of MARPOL 73/78 Annex VI on reducing the SO_2 emissions of marine. The Annex VI introduced a worldwide limit on the sulfur content of 0.5 percent to marine fuels and a limit of 0.1 percent in designated SO_2 emission control areas (SECA) from 2020[8]. Besides, in addition to the requirement of MARPOL 73/78 Annex VI Regulations, further regional requirements for the use of low-sulfur fuel are in effect, such as European Union[9], United States [10] and China[11].

Commonly speaking, there are two ways to meet the requirements of sulfur emission regulations[12]: one way is to use low-sulfur oil or other alternative fuels like liquid nature gas (LNG). The other way is to install the exhaust gas cleaning system (EGCS). Although using low-sulfur oil or other alternative fuels is an effective source control method, the cost of low-sulfur oil and other alternative fuels are far higher than the marine heavy oil[13], which will significantly increase the operating cost of large vessels. According to a research of Finland government, the cost

* Corresponding authors at: State Key Lab of Clean Energy Utilization, State Environmental Protection Center for Coal-Fired Air Pollution Control, Zhejiang University, Hangzhou 310027, China.
E-mail addresses: 11527077@zju.edu.cn (Y. Yang), zhengch2003@zju.edu.cn (C. Zheng).

https://doi.org/10.1016/j.seppur.2022.120557
Received 13 December 2021; Received in revised form 14 January 2022; Accepted 20 January 2022
Available online 24 January 2022

Nomenclature

a	specific area between gas and liquid phase, m^2/m^3
c	concentration in liquid phase, mol/m^3
c_i	concentration at the gas-liquid interface, mol/m^3
$\bar{c}$	average concentration in liquid phase during a period of time, mol/m^3
C_D	drag coefficient
d_l	diameter of droplet, m
D_g	molecular diffusivity of species in the gas phase, m^2/s
D_l	molecular diffusivity of species in the liquid phase, m^2/s
g	gravitational acceleration, N/kg
G	gas flow rate, m^3/s
H	Henry's constant, $(Pa{\cdot}m^3)/mol$
k_g	gas phase mass transfer coefficient, $mol/(m^2{\cdot}s{\cdot}Pa)$
k_{s1}	equilibrium constant of $SO_2(aq)$
k_{s2}	equilibrium constant of HSO_3^-
k_{c1}	equilibrium constant of $CO_2(aq)$
k_{c2}	equilibrium constant of HCO_3^-
k_w	equilibrium constant of H_2O
k_d	crystallization or dissolution constant, $mol/(m^3{\cdot}s)$
k_{SP}	solubility product, $(mol/m^3)^2$
L	liquid flow rate, m^3/s
N	mass transfer rate $mol/(m^3{\cdot}s)$
p	partial pressure in the gas phase, Pa
p_i	partial pressure at the gas-liquid interface, Pa
R	universal gas constant, 8.3141 J/(mol Â· K)
Re	Reynold number
RS	degree of supersaturation
r	the distance from the center of the droplet, m
r_d	dissolution reaction rate, $mol/(m^3{\cdot}s)$
S	cross-sectional area of the scrubber, m^2
Sh	Sherwood number
Sc	Schmidt number
t	movement duration of drops, s
t_p	corresponding time scale of oscillation, s
T	temperature, K
u	velocity, m/s

Greek letters

π	ratio of circumference to diameter
σ	surface tension, N/m
ρ	density, kg/m^3
μ	viscosity, Pa·s
η	efficiency, %

Subscripts

g	gas
l	liquid
abs	absorption
oxi	oxidation
$inlet$	inlet of the scrubber
dis	discharged
sea	seawater
mag	magnesium-based absorbent

increase of using low-sulfur oil will be 0.2–120 M€/year [14]. Meanwhile, marine fuel oil systems are usually designed for burning heavy oil with high sulfur contents. The general belief is that sulfur has a beneficial tribological effect due to building up of a solid lubricating film and promoting a beneficial mild corrosive wear [15]. As a result, when the fuel is switched to low-sulfur oil or LNG, the fuel system needs to be modified, which will further increase the cost. However, EGCS is a kind of flue gas desulfurization technologies, which is widely used as an effective method to deal with flue gas in SO_2 emitting industry [1,16]. Due to the reduction of additional fuel expenditure [17], the installation of EGCS is the most convenient and economic method to reduce the SO_2 emission for the ship owners in the majority of scenarios [18]. Depending on the conditions, the installation costs of EGCS can be recouped within the span of 1–2 years [2]. It provides the large vessels with an attractive alternative to the use of low-sulfur fuels, and may become more popular when the limits of sulfur emissions become tighter [19].

Marine EGCS is usually divided into open-loop EGCS, closed-loop EGCS and hybrid EGCS[18]. Among them, the hybrid system is very flexible. When the seawater alkalinity is insufficient or in SECA, it can operate in a closed loop mode to ensure enough efficiency. At the same time, when the seawater alkalinity is sufficient or outside the SECA, it can operate in open-loop mode to avoid the waste of absorbents and reduce operating costs. Therefore, hybrid EGCS have been widely used in recent years. Although the operation mode of hybrid system can be switched according to the requirement, but the operation a of hybrid EGCS is mainly based on the experience of operators, which often leads to excessive SO_2 concentration at the outlet or high operating costs, especially for routes that span multiple sea areas (the alkalinity and temperature of seawater and the emission standards may frequently change). Thus, the operation of EGCS can hardly meet the requirement of economy and safety demands. Therefore, it is necessary to modeling the SO_2 absorption process of hybrid EGCS, and explore the influence of temperature, pH, SO_2 concentration and other factors on absorption rate and desulfurization efficiency using different absorbent, and obtain control methods under different conditions, so as to realize the safe and economic operation of hybrid EGCS.

There are several kinds of materials that can be taken as the absorbents[20] such as limestone ($CaCO_3$), seawater, Sodium hydroxide (NaOH) and magnesium hydroxide ($Mg(OH)_2$)[18] etc. Many scholars paid attention to modeling the mechanism of SO_2 removal process using different kind of absorbents. In fact, calcium-based absorbent is one of the most commonly used absorbent worldwide due to its low cost and high efficiency[21]. There were plenty of studies carried out about calcium-based absorbents. For example, Brogren et al.[22] and Zhong et al. [23] were devoted to describe the SO_2 absorption process in a spray tower based on unsteady theory with numerical method. The models took limestone dissolution, sulfite oxidation, gypsum crystallization and the hydrolysis reaction of CO_2 into consideration. These models could be used to quantify the mass transfer in the spray scrubber. The influences of liquid-to-gas ratio, SO_2 concentration of inlet flue gas, and combination mode of different spray levels to the desulfurization efficiency are analyzed. Although, the calcium-based absorbents are difficult to be applied on ships due to its solid by-products and other reasons, the models are worth to be referenced. Actually, seawater is more often used as the absorbent of EGCS, rather than calcium-based absorbent. Darake et al. [24,25] and Caiazzo et al. [26] studied the reactive absorption of SO_2 in packed-bed tower and spray tower experimentally and mathematically. The influence of important factors such as flue gas temperature, flue gas velocity, droplet size, and velocity on the scrubbing process were investigated. Seawater is the absorbent of open-loop EGCS. Most closed-loop EGCS use sodium hydroxide (NaOH) as absorbent. Recent year, due to the high price of sodium hydroxide, magnesium-based absorbents are adopted by some researchers[27]. Liu et al. [28] built a CFD (computational fluid dynamic) model using R-Flow (a computational fluid dynamic software) in order to investigate the flow field and SO_2 absorption rate in the absorber of magnesium-based EGCS. The effects of liquid-gas ratio and other factors on

desulfurization efficiency were studied. The calculated results are in good agreement with the experimental values. These studies are conducted on a single kind of absorbent, which are very helpful for the design and operation of the open-loop or closed-loop EGCS. However, the hybrid EGCS can switch between the open-loop and closed-loop modes. The switching of operating mode often means the switching of absorbents. The design of hybrid EGCS is supposed to meet the desulfurization requirements of both two or even more kind of absorbents. There is still a lack of a model that can compare and study the differences on desulfurization performance among various absorbents. This poses a challenge to the design and operation of the EGCS system.

Taking the above-stated into account, a detailed model of hybrid EGCS using two different absorbents (seawater and magnesium-based absorbent) is developed. The motion of droplets, the absorption or desorption of SO_2 and CO_2, the mass transfer in the liquid phase, the dissolution or crystallization of $MgCO_3$,$MgSO_3$ and $Mg(OH)_2$, the equilibrium of the ion and charge are taken into consideration. Based on the model, the SO_2 absorption process and the crystallization process are analyzed. And then the distribution of process parameters in EGCS is achieved. Meanwhile, the desulfurization efficiency of open-loop mode and closed-loop mode under different pH, temperatures, liquid-to-gas ratios and inlet SO_2 concentration are calculated. On this basis, an operation strategy of the EGCS for different absorbents and sea areas is proposed. These results will be helpful for the design and the operation of the EGCS.

2. Model development

2.1. Process description

As mentioned above, the hybrid EGCS is a complex, but flexible technology, allowing to be switched between open-loop mode or closed-loop mode depending on the situation. A typical hybrid EGCS is shown in Fig. 1.

When the EGCS is operated as open-loop mode, the seawater is always used as absorbent. The SO_2 absorption process mainly occurs in the scrubber. The seawater sprays out from the nozzle and fully contact with the exhaust gas and remove the SO_2 from the flue gas. After absorbing SO_2, the waste water will be discharged directly into the sea. When the EGCS is operated as closed-loop mode, the NaOH or $Mg(OH)_2$ is always used as absorbent. Different from the open loop mode, the fresh absorbent will not be directly sprayed into the spray tower, but will be added to a recycle tank. What's more, the absorbent will not be discharged directly into the sea after contact with the exhaust gas, but will return into the recycle tank again and fully mixed with the fresh absorbent. The absorbent stored in the recycle tank will not be discharged until meeting certain conditions (such as high enough density or high enough liquid level). The discharged absorbent is supposed to go through the water treatment unit in order to meet the standard.

Therefore, in this paper, based on the above system, considering the motion of the droplet and the mass transfer and reaction process, an SO_2 absorption model of the hybrid EGCS system is established, which is shown in Fig. 2.

The partial processes of the EGCS using different absorbents in the scrubber can be classified as follows:

(1) For the seawater absorbents:

$$SO_2(g) \leftrightharpoons SO_2(aq)$$

$$SO_2(aq) + H_2O \leftrightharpoons HSO_3^- + H^+$$

$$HSO_3^- \leftrightharpoons SO_3^{2-} + H^+$$

$$CO_3^{2-} + H^+ \leftrightharpoons HCO_3^-$$

$$HCO_3^- + H^+ \leftrightharpoons CO_2(aq) + H_2O$$

$$CO_2(aq) \leftrightharpoons CO_2(g)$$

(2) For the magnesium-based absorbents:

$$SO_2(g) \leftrightharpoons SO_2(aq)$$

$$SO_2(aq) + H_2O \leftrightharpoons HSO_3^- + H^+$$

$$HSO_3^- \leftrightharpoons SO_3^{2-} + H^+$$

$$Mg(OH)_2(s) \leftrightharpoons Mg^{2+} + 2OH^-$$

$$Mg^{2+} + SO_3^{2-} \leftrightharpoons MgSO_3(s)$$

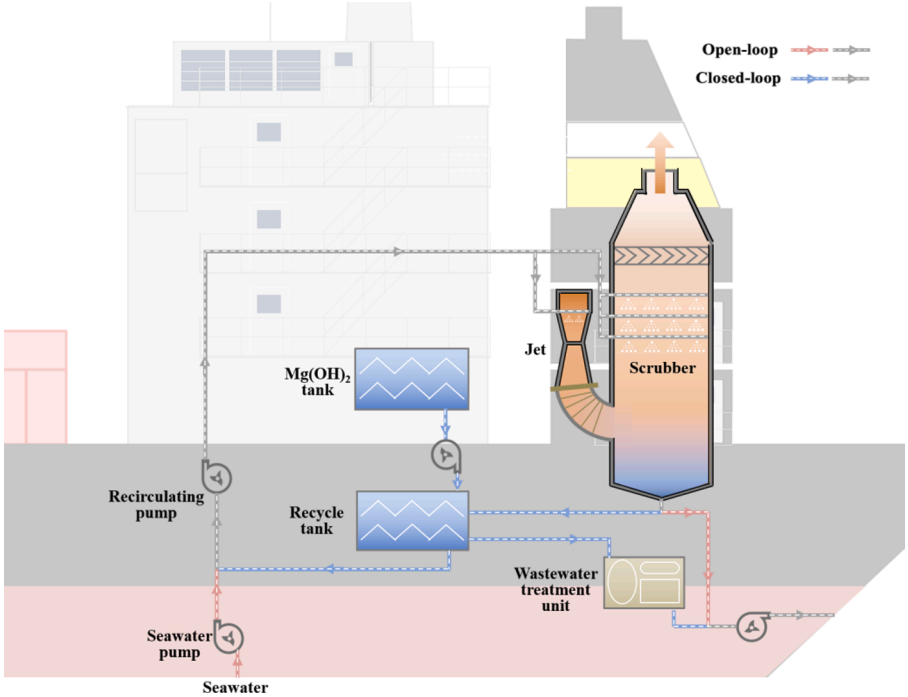

Fig. 1. Diagrammatic sketch of a typical hybrid EGCS.

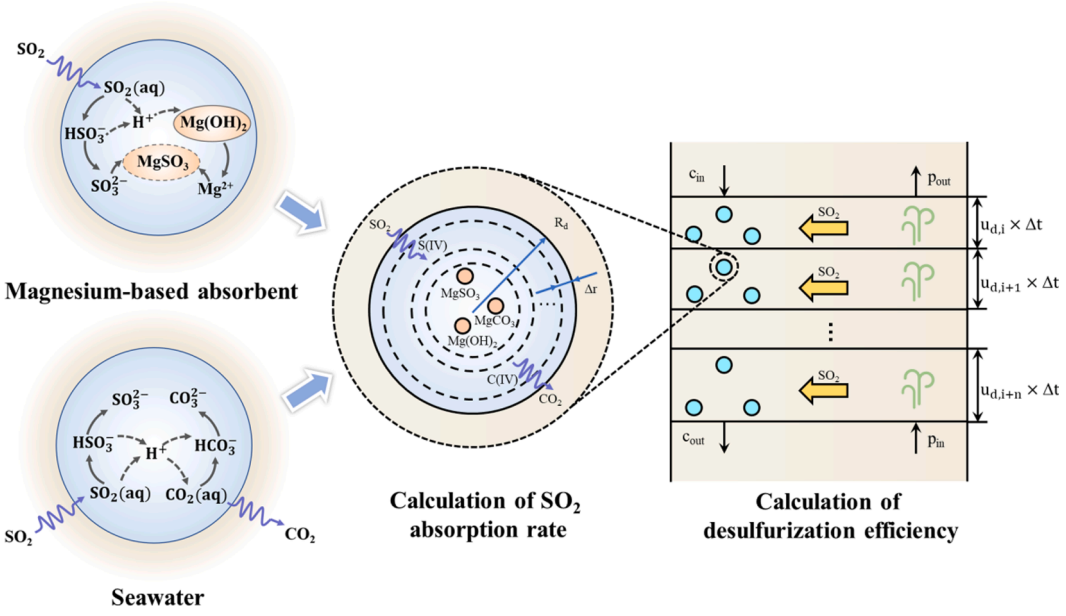

Fig. 2. Diagram of calculation process in the numerical model.

$$H^+ + OH^- \leftrightharpoons H_2O$$

The absorption zone has been discretized into n calculation cells numbered from top (i = 1) to bottom (i = n), and the droplets have been discretized into m calculation cells from the surface (j = 1) to the center (j = n) of the droplets.

2.2. Assumptions

Since the procedures in EGCS are considerably complex, such as collisions between droplets, gas-liquid distribution in scrubber, collision between droplets and scrubber sidewalls, etc. It's hard to describe all the procedures critically with the numerical method. The following assumptions are thus made for the model:

1. The flue gas is regarded as an ideal gas. The volume of flue gas is not influenced by mass transfer. The temperature is the same between gas and liquid phase.
2. The droplets are considered to be a standard sphere with the same size. All droplets are evenly distributed on the horizontal plane. There is no collision between droplets.
3. The charge balance and ion balance are instantaneously reached in the droplets.
4. Only the effects of H^+, OH^-, Mg^{2+}, S(IV) and C(IV) are considered in the calculation of SO_2 absorption process

2.3. Numerical model

The main reactor of the hybrid EGCS is the scrubber. In the scrubber, the seawater and the magnesium-based absorbent contact with the exhaust gas and absorb the SO_2. In order to build a detailed model, the SO_2 removal process in the scrubber, the following process are taken into the consideration.

2.3.1. Motion of droplets

The motion of droplets can be described by the balance of forces acting, which can be express by Eq. (1)[29]:

$$\frac{\pi}{6}d^3\rho_l\frac{du_l}{dt} = \frac{\pi}{6}d^3(\rho_l - \rho_g)g - C_D\rho_g\frac{\pi}{4}d^2\frac{(u_g - u_l)^2}{2} \quad (1)$$

where C_D is the drag coefficient and can be calculated by Eq. (2) and (3):

$$C_D = \frac{24}{Re}(1 + 0.125Re^{0.72}) \quad (2)$$

$$Re = \frac{d|u_g - u_l|\rho_g}{\mu_g} \quad (3)$$

And the specific area between gas and liquid phase can be obtained by Eq. (4)

$$a = \frac{6L}{dSu_l} \quad (4)$$

2.3.2. Mass transfer and reaction

Absorption or desorption and of SO_2 and CO_2: When the EGCS is operated in open-loop mode, the droplets absorb SO_2 from exhaust gas and release CO_2 at the same time. When the EGCS is operated in closed-loop mode, droplets absorb SO_2 from exhaust gas. The absorption or desorption rate of SO_2 and CO_2 can be defined by calculating the flux of SO_2 and CO_2 [30]:

$$N_A = k_{g,A}(p_A - p_{i,A}) \quad (5)$$

Here, A is the gaseous solute such as SO_2 or CO_2.

And the gas phase coefficient $k_{g,A}$ can be acquired by Frösslling correlation[31]:

$$Sh = \frac{k_{g,A}dRT}{D_{g,A}} = 2 + 0.55Re^{0.5}Sc^{1/3} \quad (6)$$

where Sc is the Schmidt number:

$$Sc = \frac{\mu_g}{\rho_g D_{g,A}} \quad (7)$$

The gas phase diffusion coefficient can be predicted by FSG method, expressed by Fuller et.al[32]:

$$D_{g,A} = \frac{9.86 \times 10^{-9} \cdot T^{1.75} \cdot \left[\frac{1}{M_{air}} + \frac{1}{M_A}\right]^{1/2}}{0.000001 \cdot p \cdot \left(V_{air}^{1/3} + V_A^{1/3}\right)^2} \quad (8)$$

The pressure of exhaust gas is close to 1 atm, the concentration of SO_2 is low (several hundred ppm). As a result, at the gas-liquid interface, the partial pressure of gas can be calculated by Henry's law:

$$p_{i,A} = Hc_{i,A} \tag{9}$$

Mass transfer in the liquid phase: According to the Fick's law, such unsteady mass transfer with chemical reaction process can be described as [23]:

$$\frac{\partial c_A}{\partial t} = \sum_{i=1}^{n} D_{A_i}\left(\frac{\partial^2 c_{A_i}}{\partial r^2} + \frac{2}{r}\frac{\partial c_{A_i}}{\partial r}\right) - r_{d,A} \tag{10}$$

Here, A is the species in the slurry such as S(IV), C(IV), Mg(II) etc.

Dissolution or crystallization of $MgCO_3$,$MgSO_3$ and $Mg(OH)_2$: The dissolution or crystallization of $MgCO_3$,$MgSO_3$ and $Mg(OH)_2$ can be described by Eq. (10).

$$r_d = k_d(RS - 1) \tag{11}$$

where the degree of supersaturation of $MgCO_3$,$MgSO_3$ and $Mg(OH)_2$ are shown in the Table 1.

Equilibrium of the ion and charge: According to the ionic equilibrium theory, the equilibrium constants of S(IV), C(IV), S(VI) and H_2O are shown in the Table 2.

The equilibrium constants mentioned above are calculated based on the work of Pasiuk-Bronikowska and Rudziński[33].

With the assumption 3, the charge equilibrium can be described as flowing:

$$c_{H^+} - c_{OH^-} 2c_{Mg^{2+}} - 2c_{SO_3^{2-}} - c_{HSO_3^-} - 2c_{CO_3^{2-}} - c_{HCO_3^-} = 0 \tag{12}$$

According to the works of Angelo et. al[34], during the falling process of droplets, the droplet will oscillate between an oblate spheroid and a prolate spheroid during the falling process. The corresponding time scale can be calculated as follows:

$$t_p = \frac{\pi}{4}\sqrt{\frac{\rho_l d^3}{\sigma_l}} \tag{13}$$

After each oscillation, the contents of the droplet mix completely, and the average concentration of each contents in the droplet will be calculated and then replace the present value, which will modify the errors caused by the inner circulation in the droplets.

Since the absorption in the absorber is countercurrent, the boundary conditions are separated. The initial content of the droplet is known at the top of the scrubber. However, the content of the flue gas at the top of the scrubber is not clear. As a result, it is necessary to calculate the SO_2 partial pressure from the top to the bottom with the assumed outlet SO_2 partial pressure in order to obtain the inlet SO_2 partial pressure, and continuously amend outlet SO_2 partial pressure by the dichotomy method. Finally, an accurate outlet SO_2 partial pressure can be obtained. The strategy of the calculation program is shown as Fig. 3. The model is programed and realized based on the MATLAB 2020.

3. Results and discussion

In this part, the SO_2 absorption rate mentioned is regard to the mass transfer rate of SO_2 from flue gas to the droplets of seawater and magnesium-based absorbent. And the mass transfer coefficient regard to the SO_2 absorption ability of the droplets.

Table 1
The degree of supersaturation of **$MgCO_3$**,**$MgSO_3$** and.**$Mg(OH)_2$**

Symbol	Explanation	Equations
RS_{MgCO_3}	Degree of supersaturation of $MgCO_3$	$c_{Mg^{2+}}c_{CO_3^{2-}}/k_{SP,MgCO_3}$
RS_{MgSO_3}	Degree of supersaturation of $MgSO_3$	$c_{Mg^{2+}}c_{SO_3^{2-}}/k_{SP,MgSO_3}$
$RS_{Mg(OH)_2}$	Degree of supersaturation of $Mg(OH)_2$	$c_{Mg^{2+}}c^2_{OH^-}/k_{SP,Mg(OH)_2}$

Table 2
Equilibrium constant of S(IV), C(IV), S(VI) and H_2O.

Symbol	Explanation	Equations
k_{s1}	Equilibrium constant of SO_2(aq)	$c_{H^+}c_{HSO_3^-}/c_{SO_2(aq)}$
k_{s2}	Equilibrium constant of HSO_3^-	$c_{H^+}c_{SO_3^{2-}}/c_{HSO_3^-}$
k_{c1}	Equilibrium constant of CO_2(aq)	$c_{H^+}c_{HCO_3^-}/c_{CO_2(aq)}$
k_{c2}	Equilibrium constant of HCO_3^-	$c_{H^+}c_{CO_3^{2-}}/c_{HCO_3^-}$
k_w	Equilibrium constant of H_2O	c_{H^+}Â·c_{OH^-}

3.1. Model validation

Several groups of test data from EGCS of 2 ships under different loads are used to verify the numerical model. The main engines are 51.5 MW and 19.8 MW, respectively. The operation conditions of the ships are shown in Table 3. Fig. 4 shows the calculated efficiency versus the measured efficiency. The average error between calculated efficiency and the measured efficiency is 2.26 ppm and the largest error is 9.9 ppm. Meanwhile, the trend of calculated value matches the measured value. The comparison reveals that the model can describe the SO_2 absorption process in the EGCS well.

3.2. SO_2 absorption process in the droplet

In hybrid EGCS, two or more different kinds of absorbents are used. Different kinds of absorbents usually have different SO_2 absorption performance. This is a challenge for the operation of the hybrid EGCS system. In this part, based on the model mentioned above, the SO_2 absorption process in the droplet of two typical kinds of absorbents are compared, and the influence of important factors of SO_2 absorption rate and crystallization performance are obtained.

3.2.1. SO_2 absorption rate

Generally speaking, the key factors affecting SO_2 absorption process are pH, temperature and droplet composition.

Influence of pH: The pH of the absorbent is always considered to be an important parameter during the SO_2 absorption process. Fig. 5 shows the effects of pH value on the SO_2 absorption rate and mass transfer coefficient of seawater and magnesium-based absorbent.

The pH of seawater is usually depended on its alkalinity, while the pH of magnesium-based absorbent is usually depended on the $Mg(OH)_2$/SO_2 ratio. As shown in Fig. 5 **(a)**, for magnesium-based absorbent, the pH is related to the exist form of S(IV) and also affects the dissolution rate of $Mg(OH)_2$. For seawater, the pH affects the distribution of S(IV) and C(IV) in the liquid phase, thus affecting the absorption of SO_2 and the desorption of CO_2. The effects of pH value on SO_2 absorption rate are shown in Fig. 5 **(b)**.

According to Fig. 5 **(b)**, with the increase of pH, the absorption rate of both seawater and magnesium-based absorbent increase. Meanwhile, higher SO_2 concentration usually led to higher SO_2 absorption rate for both of two absorbents. When the S(IV) concentration of magnesium-based absorbent is 0 mol/m^3, the effect of pH on the SO_2 absorption rate is similar to seawater. However, when the S(IV) concentration is 100 mol/m^3 or 200 mol/m^3, with the increase of pH, the SO_2 absorption rate increases rapidly first and then gradually slows down, which is significantly different with the seawater.

In order to explain the reason of different variation of SO_2 absorption rate with pH between seawater and magnesium-based absorbent, Fig. 5 **(c)** shows the effects of pH on mass transfer coefficient. With the increase of pH, the mass transfer coefficient of both seawater and magnesium-based absorbent increase. Obviously, the pH value of the absorbent can only affect the mass transfer and reaction process in the liquid phase. As the pH increases, the reaction rate of SO_2 in the liquid phase increases, and the mass transfer coefficient the liquid phase increases, resulting in an increase in the overall mass transfer coefficient.

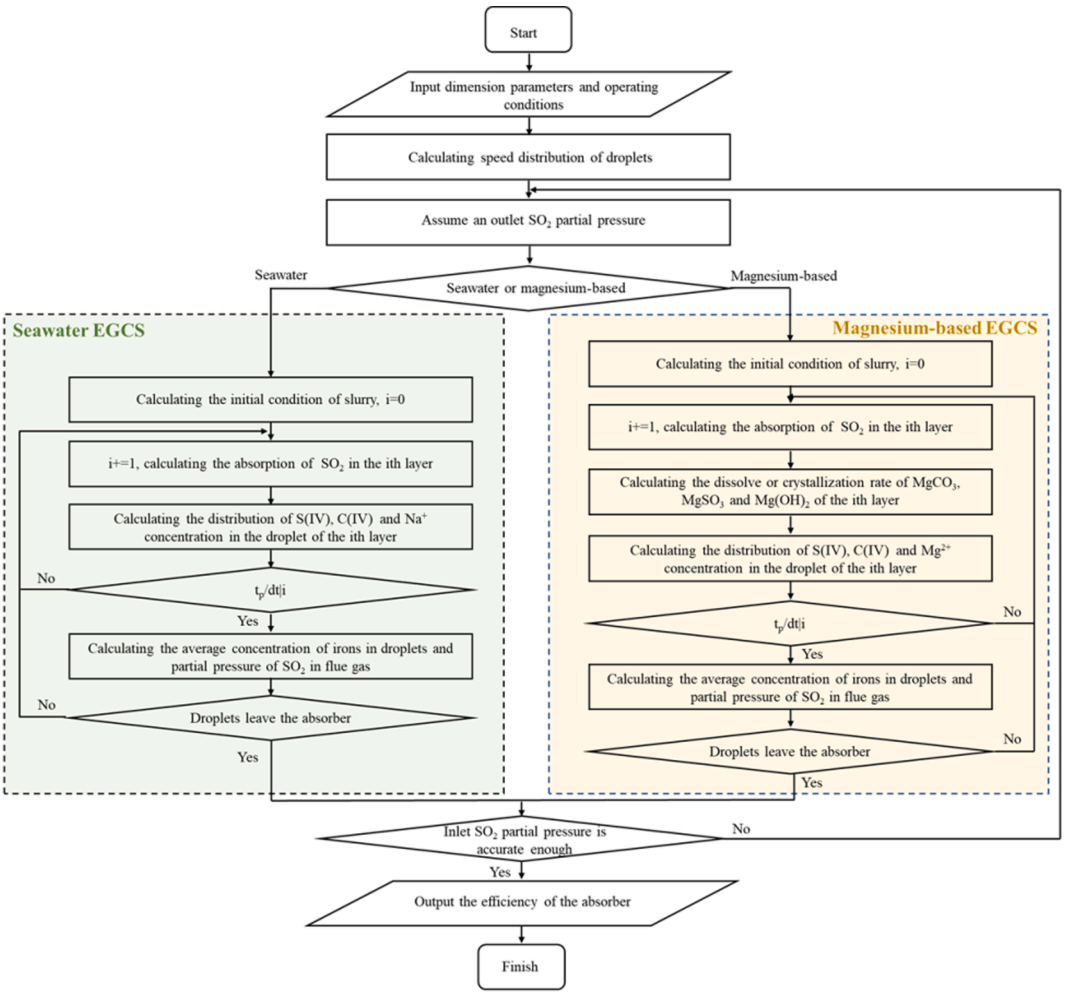

Fig. 3. The strategy of calculation.

Table 3
Operation conditions of the ships used for validation.

	Sulfur content (%)	Load (%)	Mode	Inlet CO_2(%)	Inlet SO_2 (ppm)	Temperature (°C)	pH	Washwater flow rate (L/h)
Ship 1	2.8	50	closed	3.55	433.430	48	6.61	754
		50	closed	3.55	433.430	37	6.32	681
		85	closed	3.6	439.535	52	6.8	768
		85	closed	3.58	437.093	55	6.36	708
		50	open	3.49	426.105	9	7.8	469
		50	open	3.48	424.884	9	7.9	518
		85	open	3.6	439.535	9	7.8	541
		85	open	3.61	440.756	10	7.9	479
Ship 2	2.28	50	closed	4.73	458.780	56	6.51	2116
		50	closed	4.67	452.961	55	6.9	1769.2
		60	closed	4.67	452.961	27	7	2114
		60	closed	4.72	457.811	46	6.79	1989
		50	open	4.74	459.750	13	8.1	1263
		50	open	4.84	469.450	13	7.9	968
		60	open	4.56	442.292	12	8	1320
		60	open	4.59	445.201	12	7.4	997

However, when the concentration of S(IV) is high, S(IV) can be regarded as a pH buffer, slowing down the accumulation rate of SO_2(aq), thereby increasing the liquid phase mass transfer coefficient as well. When the liquid phase mass transfer coefficient is large enough, the absorption process is controlled by the gas phase mass transfer. The gas phase transfer coefficient limits the further increase of the total mass transfer coefficient.

What's more, in Fig. 5 **(b)**, when the pH is low, the higher S(IV) concentration will significantly increase the SO_2 absorption rate of magnesium-based absorbent. However, when the pH is high, the SO_2 absorption rate will decrease with the increase of S(IV) concentration. According to the Fig. 5 **(c)**, when the pH is low, the S(IV) stabilizes the pH, and thus increase the mass transfer coefficient. However, when the liquid phase mass transfer coefficient is large enough, the absorption process is controlled by the mass transfer in gas phase. At this time, further improve the S(IV) concentration will reduce the driving force of mass transfer process, thus reduce the absorption rate.

Influence of temperature: In addition to pH, temperature is also a

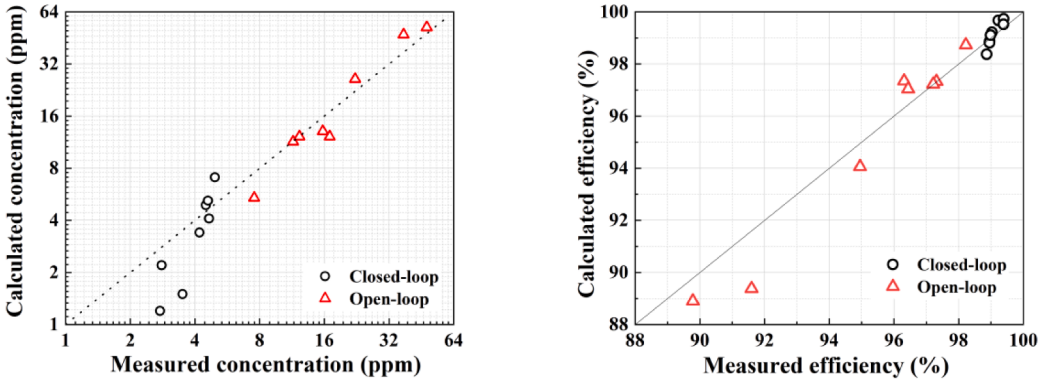

(a) outlet SO_2 concentration (b) SO_2 removal efficienty

Fig. 4. Comparisons between calculated value and measured value.

key factor affecting the absorption rate of SO_2. Fig. 6 shows the effects of temperature on the SO_2 absorption rate and mass transfer coefficient of seawater and magnesium-based absorbent.

There are three reasons why temperature can affect the absorption rate, as shown in Fig. 6 **(a)**. The first reason is that the temperature can affect the diffusion coefficient in the gas phase and liquid phase. Higher temperature will promote the mass transfer process. The second reason is that the temperature can affect the Henry's constant. The solubility of the gaseous solute closely depends on the temperature. With the increase of temperature, the solubility of the gaseous solute decrease. The third reason is that the temperature can affect the reaction rate during the SO_2 absorption process. The chemical reaction rate of the SO_2 absorption process will change with the temperature.

As shown in Fig. 6 **(b)**, when the S(IV) concentration is 0 mol/m^3, the absorption rate of magnesium-based absorbent varies with the temperature is similar to seawater, and the absorption rate decreases with the increase of temperature. However, when S(IV) concentration is 100 mol/m^3 or 200 mol/m^3, the effects of temperature on absorption rate and mass transfer coefficient are quite different from seawater. When the temperature is less than 50 °C, the temperature has little effect on the absorption rate. It is worth mentioning that when the concentration of S (IV) is 100 mol/m^3 and the concentration of SO_2 is 2000 mg/m^3, the absorption rate reaches the maximum when the temperature is equal to 32 °C. Moreover, under the condition that the SO_2 concentration is 2000 mg/m^3, when the temperature is higher than 65 °C, the SO_2 absorption rate decreases with the increase of S(IV) concentration. While, when the temperature is lower than 65 °C, the absorption rate increases with the S (IV) concentration.

Fig. 6 **(c)** shows the effects of temperature on mass transfer coefficient. Similarly, when the S(IV) concentration is fixed at 0 mol/m^3, the trend of mass transfer coefficient of magnesium-based absorbent varies with the temperature is similar to seawater, and the mass transfer coefficient decrease with the increase of temperature. When the concentration of S(IV) is 100 mol/m^3 and the concentration of SO_2 is 2000 mg/m^3, the mass transfer coefficient reaches the maximum when the temperature is equal to 35 °C. When the concentration of S(IV) is 100 mol/m^3 and the concentration of SO_2 is 3000 mg/m^3, the mass transfer coefficient reaches the maximum when the temperature is equal to 30 °C. Also, according to Fig. 6 **(c)**, the phenomenon mentioned above can be explained. When the temperature is lower than 65 °C, increasing S(IV) will increase the reaction rate of SO_2(aq) and the diffusion rate of matters, and thus improve the mass transfer coefficient. When the temperature is higher than 65 °C, improving the concentration of S(IV) will reduce the driving force of mass transfer process, thus reduce the SO_2 absorption rate.

3.2.2. *Crystallization performance*

In the hybrid EGCS, the crystallization process will cause scaling problems in the scrubber and the recycle tank, thereby jeopardizing the safety of the EGCS system. It can be seen from Fig. 5 **(a)** that when the S (IV) concentration is fixed to 200 mol/m^3, the situation of pH > 6.55 is not calculated. This is because when the S(IV) concentration is 200 mol/m^3 and pH is>6.55, the $MgSO_3$ in the slurry will crystallize so that the composition of the absorbent will be changed in order to rebuild the dissolution balance. In fact, in addition to $MgSO_3$, $MgCO_3$ also exists in the deposition of the magnesium-based desulfurization system. Therefore, for magnesium-based absorbents, the crystallization characteristic of $MgSO_3$ and $MgCO_3$ should also be studied to avoid scrubber and recycle tank from scaling.

Fig. 7 shows the effects of pH value and temperature on the crystallization in magnesium-based EGCS. With the increase of pH, the critical crystallization concentration of both $MgSO_3$ and $MgCO_3$ decreases. With the increase of temperature, the crystallization S(IV) concentration of both $MgSO_3$ and $MgCO_3$ increases. The crystallization of $MgCO_3$ may occur only if the pH of the magnesium-based absorbent is too high. However, in order to prevent crystallization of $MgSO_3$, it is necessary to control the pH, temperature and S(IV) concentration of the magnesium-based absorbent at the same time.

3.3. *SO_2 absorption process in the scrubber*

The scrubber is most commonly used in the marine EGCS especially in hybrid EGCS. In the scrubber, the droplets are ejected from the nozzle and contact with the exhaust gas. In sections 3.2, the key factors affecting the absorption and crystallization process in the droplet are mainly studied. As the droplets fall, the SO_2 will be absorbed by the droplets, thereby decreasing the pH and increasing the S(IV) concentration in the droplets. Meanwhile, the SO_2 concentration of the flue gas will be obviously changed. Due to the mass transfer between the gas and the droplets, the factors will vary as the droplets fall. Different absorbents have different desulfurization characteristics, and the distributions of process parameters with the height of the spray zone are also different. The distribution of key process parameters in EGCS under typical working conditions is studied, which is shown in Fig. 8.

As can be seen from the Fig. 8, there is an obvious difference between seawater and magnesium-based absorbent on the distribution of process parameters with the height of the spray zone. The pH of seawater decreases quickly as the droplets fall, while the pH of magnesium-based absorbent is much more stable and does not decrease significantly. Therefore, when the EGCS is switched to the open-loop mode and using seawater as absorbent, a higher inlet SO_2 concentration will significantly affect the desulfurization performance of EGCS. However, when the

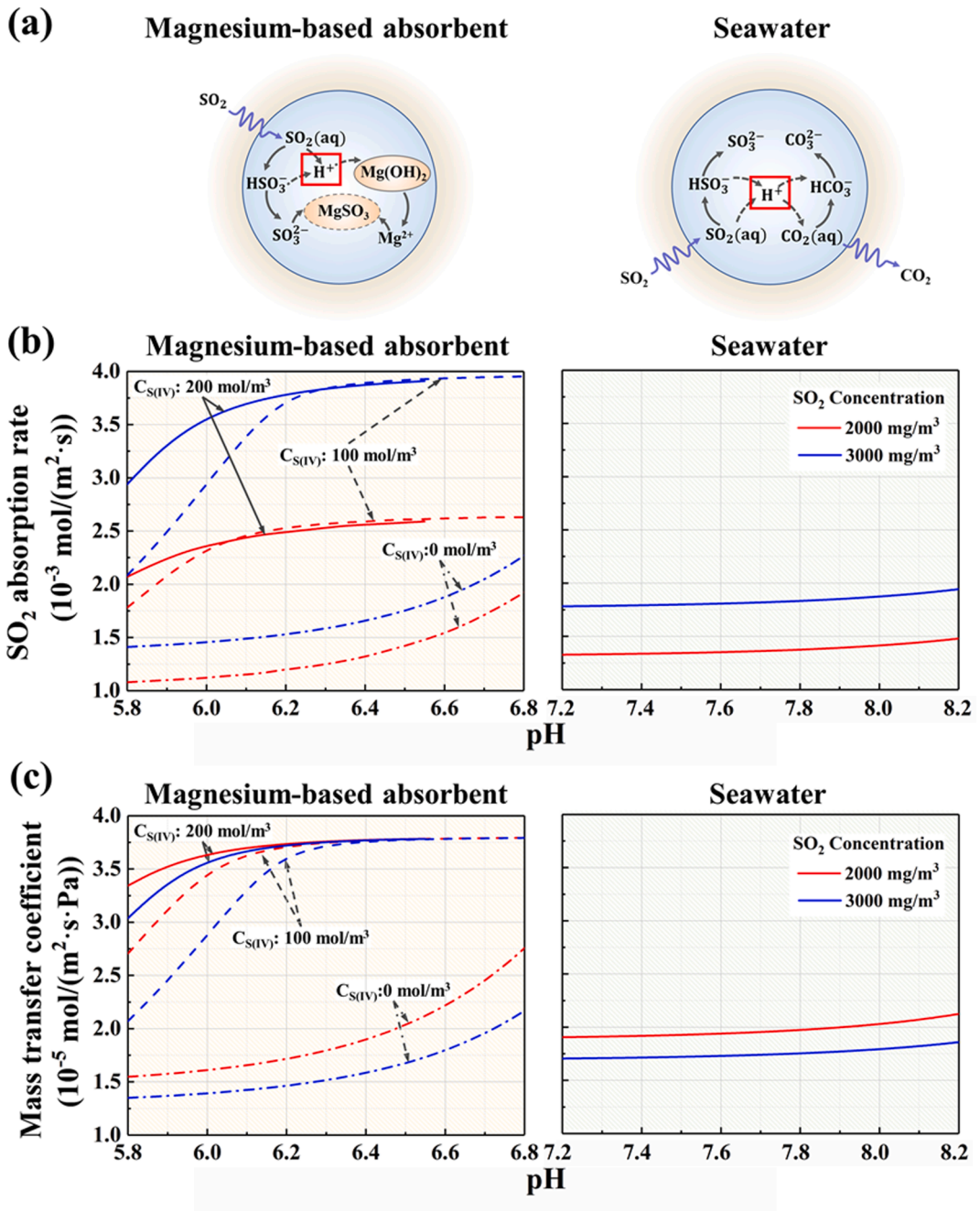

Fig. 5. **(a)** Schematic diagram of effects of pH value on SO_2 absorption process. **(b)** Effects of pH value on SO_2 absorption rate. **(c)** Effects of pH value on mass transfer coefficient. **(Temperature = 50 °C; mole ratio of CO_2 = 4.5 %; velocity between gas and liquid phase = 4 m/s).**

EGCS is switched to the closed-loop mode, there is almost no difference between the pH of droplets at the top and bottom of the scrubber. Thus, the magnesium-based absorbent shows a better adaptability to the inlet SO_2 concentration.

What's more, there is a maximum SO_2 absorption rate of the seawater as the droplets fall, which is quite different from that of magnesium-based absorbent. In general, the variation of absorption rate in the scrubber is mainly caused by the change of mass transfer driving force and the change of mass transfer coefficient. In most cases, as the droplet falls, the mass transfer driving force will gradually increase due to the increase of SO_2 concentration in the flue gas, while the mass transfer coefficient will gradually decrease due to the change of pH value. At the top of the scrubber. The SO_2 absorption rate of seawater increases with the increase of the mass transfer driving force. While, at the bottom of the scrubber, the change of seawater pH will significantly affect the SO_2 absorption rate. As the pH gradually decreased, the absorption rate also decreased gradually. However, the pH of magnesium-based absorbent is much more stable and does not decrease significantly. As a result, with the monotonous change of the driving force of mass transfer, the absorption rate also changes monotonically.

3.4. Operation strategy of EGCS for safety and efficiency

In the actual operation process, the timely switching of the operating mode is very important. Generally speaking, the EGCS operation mode is switched according to the position the location of the ship and whether the export S/C (ratio of volume fraction SO_2 and CO_2, ppm/%) meets the standard. However, this is difficult to guarantee the safety and efficiency of the system. In fact, to determine whether the operation mode should be switched should also consider a series of parameters such as the pH

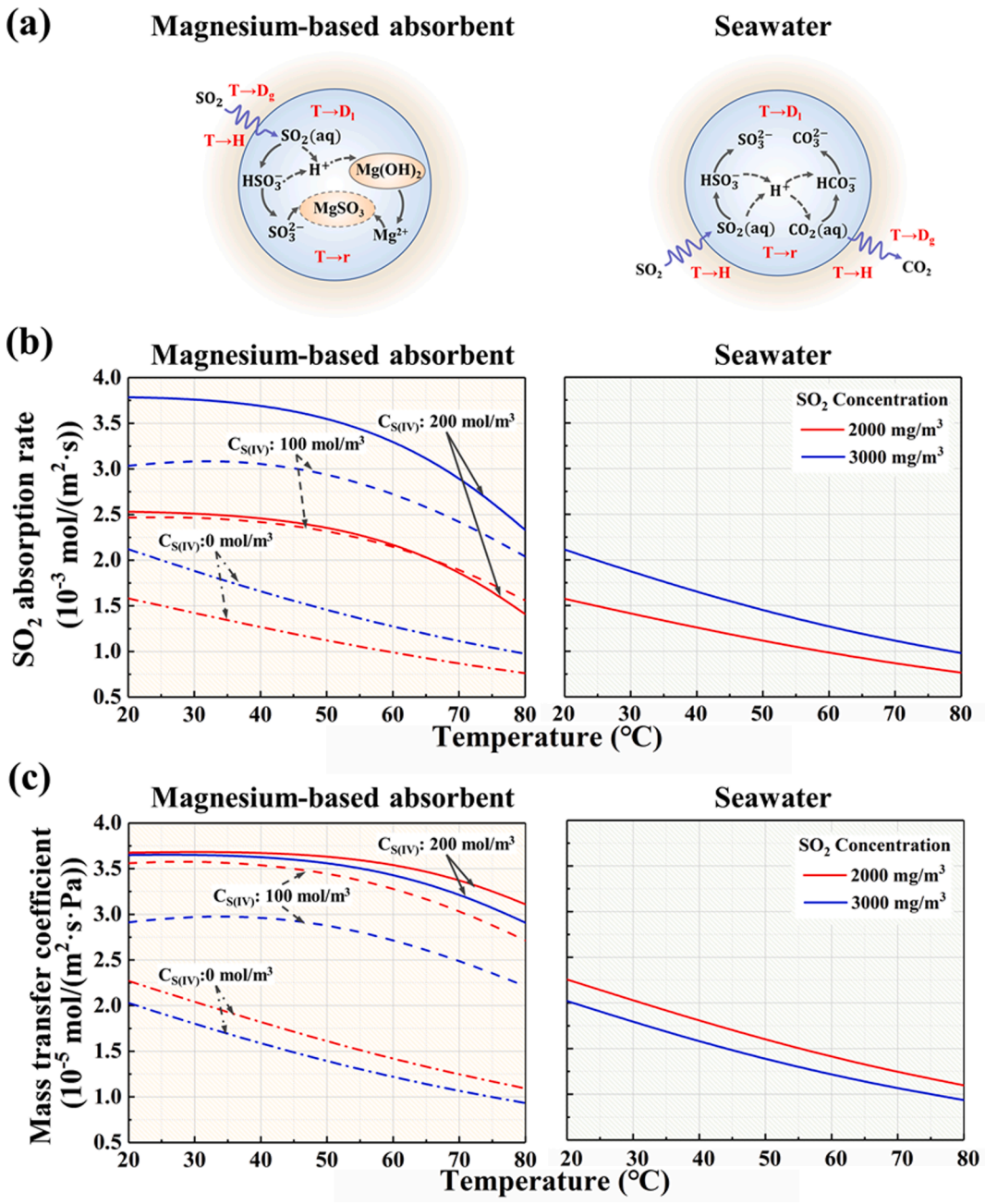

Fig. 6. **(a)** Schematic diagram of effects of temperature on SO_2 absorption process. **(b)** Effects of temperature on SO_2 absorption rate. **(c)** Effects of temperature on mass transfer coefficient. **(pH_{sea} = 8; pH_{mag} = 6.8; mole ratio of CO_2 = 4.5 %; velocity between gas and liquid phase = 4 m/s)**.

and temperature of the seawater. Thus, in this part, the operation strategy of EGCS for safety and efficiency is discussed.

3.4.1. *Operation strategy for safety*

First of all, the most important thing is to ensure the safe operation of EGCS. Scaling will greatly affect the safety of EGCS, especially it is operated in closed-loop mode. According to Fig. 7, the $MgCO_3$ will crystallize only if the pH value is higher than 7.2. Therefore, under normal operating conditions, $MgSO_3$ is more likely to cause scaling. In the condition of continuous slurry discharge, the average S(IV) concentration in the slurry during a period of time can be described as:

$$\overline{c}_{S(IV)} = \int_{t_1}^{t_2} \frac{G\eta_{abs}\eta_{oxi}c_{SO_2,inlet}}{M_{SO_2}L_{discharge}}dt \tag{14}$$

It is possible to determine whether or not crystallization will occur under the condition of different inlet SO_2 concentrations and pH values, so as to prevent the absorber or recycle tank from scaling, which is shown in Fig. 9. Under the condition of a certain inlet concentration, the EGCS can be prevented from scaling by increasing the flowrate of slurry discharge, decreasing the pH of the slurry, and enhancing the oxidation.

3.4.2. *Operation strategy for efficiency*

On the premise of ensuring the safe operation of EGCS, it is necessary to reduce the operating cost of EGCS and prevent the outlet S/C from over-standard. Due to the large fluctuations in seawater temperature and pH on a global scale [35–37], as shown in Fig. 10 **(a)**, the important influencing parameters such as temperature, pH and liquid–gas ratio (L/G) on the desulfurization efficiency of seawater and magnesium desulfurization are studied, and the results are shown in Fig. 10 **(b)** and **(c)**. As shown in Fig. 10 **(a)**, the pH of seawater worldwide is mainly

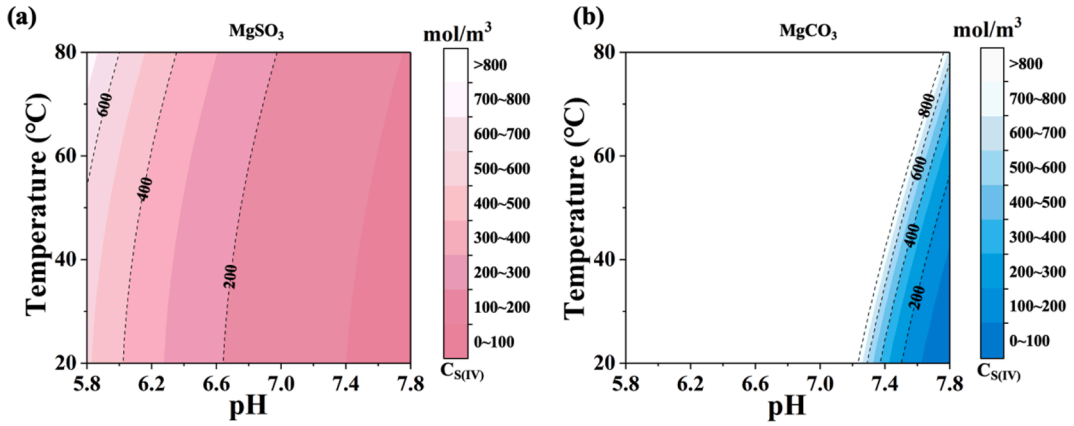

Fig. 7. Effects of pH value and temperature on the critical crystallization S(IV) concentration of **(a)** $MgSO_3$ **(b)** $MgCO_3$.

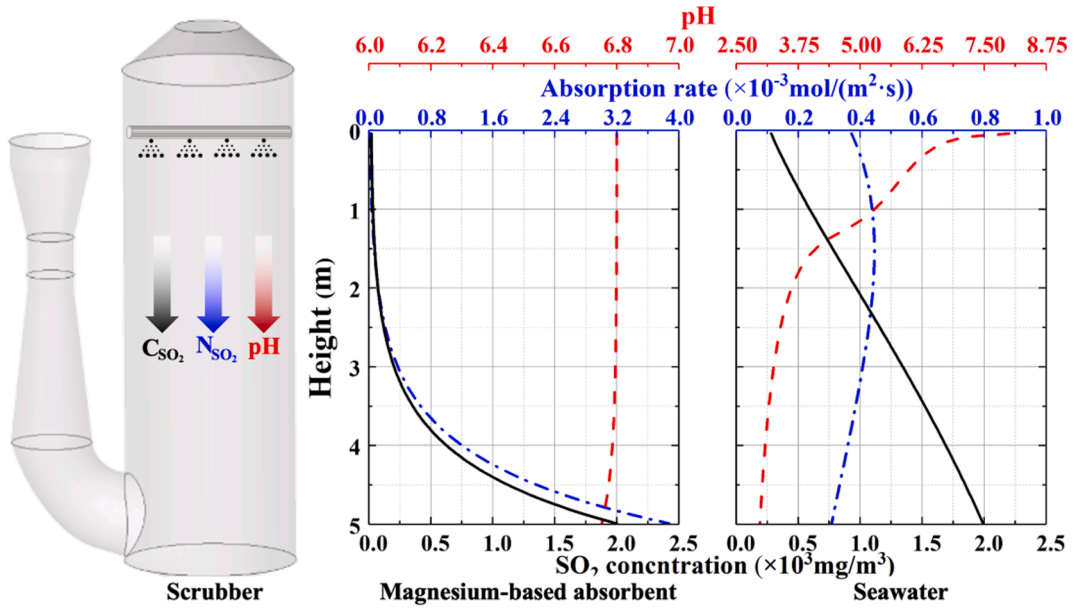

Fig. 8. Distribution of process parameters with the height of the spray zone.

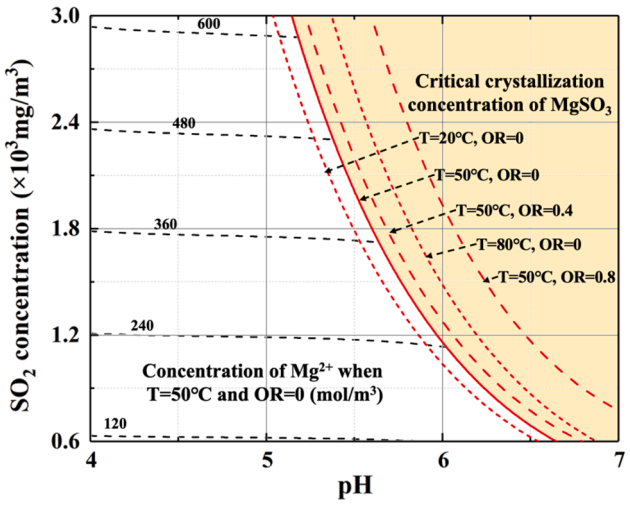

Fig. 9. Effects of pH, temperature and oxidation rate (OR, the ratio between sulfur oxidized from tetravalent to hexavalent and total absorbed sulfur) of sulfur on the critical crystallization concentration of magnesium-based absorbent.

7.5–8.25, and the temperature of seawater is mainly 0–30 °C.

As shown in Fig. 10 **(b)**, the desulfurization efficiency of open-loop mode increases with the increase of liquid–gas ratio/pH/temperature. Besides, the SO_2 removal efficiency of open-loop mode is greatly affected by the inlet SO_2 concentration. And as the inlet SO_2 concentration increases, the influence of liquid gas ratio/pH/temperature on the desulfurization efficiency gradually increases. In practical applications, the desulfurization efficiency of the open-loop mode is easily affected by inlet concentration, seawater pH, and seawater temperature. Therefore, when the inlet SO_2 concentration is higher than 2000 mg/m^3, the emission standard will never be met with open-loop mode unless the liquid gas ratio is high enough. Under these situations, using open-loop mode is not an efficient way to realize the desulfurization of the exhaust gas, especially in the SECA because of its stricter emission standards.

As shown in Fig. 10 **(c)**, the desulfurization efficiency of closed-loop mode increased with liquid gas ratio/pH/temperature as well. Compared with open-loop mode, the inlet SO_2 concentration has a relatively small effect on closed-loop mode. Not only that, the pH value of the absorbent in the closed-loop mode is controllable, which means that the closed-loop mode can adopt nearly all application scenarios. Moreover, since the efficiency of the closed-loop mode is less affected by the temperature of the absorbent, it is not necessary to equip the

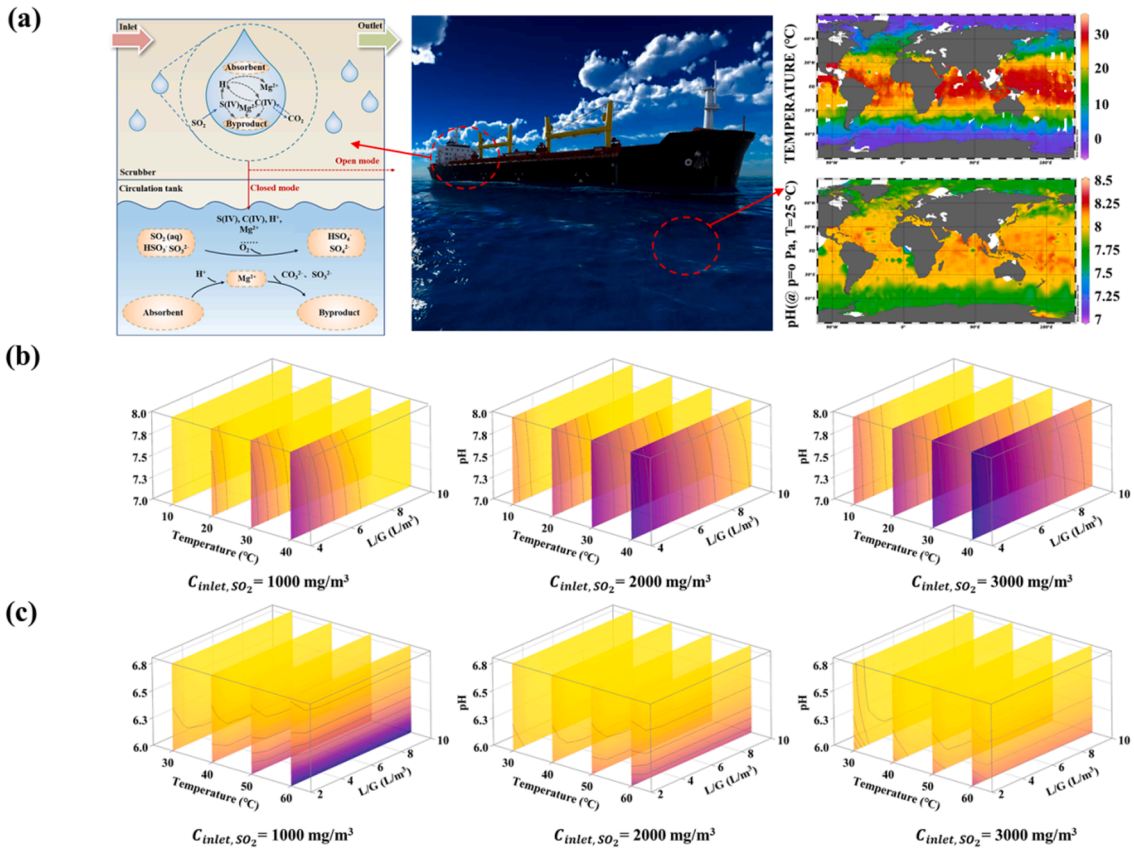

Fig. 10. Effects of temperature and pH on the desulfurization efficiency of EGCs at (b) open-loop and (c) closed-loop.

absorbent heat exchanger when using the closed-loop mode, which can further reduce the investment and operating costs of EGCS. At the same time, different from open-loop mode, the efficiency of closed-loop mode increases as the inlet SO_2 concentration increases, although the outlet SO2 concentration increase as well. This is because the desulfurization process of closed-loop mode is mainly controlled by the gas phase mass transfer. As a result, the inlet concentration has little influence on the mass transfer coefficient. At this time, the absorption rate is only related to the driving force of the mass transfer process. However, when the SO_2 concentration in the flue gas is low, the magnesium-based absorbent is difficult to remove the SO_2 from the exhaust gas due to the limitation of the mass transfer driving force. At this time, it should be switched to open mode to reduce the cost and further improve the desulfurization efficiency.

Therefore, in the actual operation process, when the pH and temperature of the seawater are measured, the minimum liquid-gas ratio that meets the emission requirements can be obtained according to Fig. 10 **(b)**. At the same time, the maximum operating pH can also be obtained under the current conditions of inlet concentration according to Fig. 9. Usually, in the closed-loop mode, the absorbent temperature will be maintained at about 50 °C. At this time, the minimum liquid-gas ratio of the closed-loop mode at the same efficiency can be obtained according to Fig. 10 **(c)**. Taking the price of the magnesium-based absorbent into consideration, the decision on whether the operating mode should be switched can be made.

4. Conclusion

In this paper, a detailed model is established of SO_2 absorption process in hybrid EGCS using seawater and magnesium-based absorbent. The motion of droplets, the absorption or desorption of SO_2 and CO_2, the mass transfer in the liquid phase, the dissolution or crystallization of $MgCO_3$,$MgSO_3$ and $Mg(OH)_2$, the equilibrium of the ion and charge are taken into consideration.

Based on the model, a comparison between seawater and magnesium-based absorbent on the SO_2 absorption process in the droplet is made. The important factors (temperature, pH, S(IV) concentration, etc.) of the absorption rate and mass transfer coefficient of different absorbents are obtained. The absorption rate of SO_2 of magnesium-based absorbent is nearly not affected by pH value and temperature under the condition of pH value $>$ 6.6 and temperature less than 50 °C. At the same time, the influence of pH and temperature on the critical crystallization concentration of magnesium method absorbent is studied. Scaling is more likely to occur when the pH is high and the temperature is low.

And then the distribution of process parameters with the height of the spray zone are obtained. It is found that the distribution of process parameters of seawater and magnesium-based absorbent are completely different, which may determine the completely different desulfurization performance of these two kinds of absorbent. Compared with seawater, the pH of magnesium-based absorbent is almost unchanged as the droplets fall. Therefore, magnesium-based absorbents are recommended when the inlet SO_2 concentration is high.

Finally, the crystallization and desulfurization performance of EGCS under different conditions are studied. In order to ensure the safe operating of EGCS and prevent the EGCS from scaling, the safe operation ranges of magnesium-based absorbent under different temperature and oxidation rate are given. And an operation strategy of the EGCS for different absorbents and sea areas is proposed. The operators can adjust the liquid-gas ratio of the current operating mode or switch to other modes according to the temperature and pH of seawater and emission standard. These results will be helpful for the design and the operation of the EGCS.

CRediT authorship contribution statement

Zhongyang Zhao: Conceptualization, Investigation, Methodology, Visualization, Validation, Writing – original draft, Writing – review & editing. **Yongxin Zhang:** Investigation, Methodology. **Yuhao Shao:** Investigation, Methodology. **Chang Liu:** Investigation. **Wenjun Li:** Investigation. **Haidong Fan:** Validation. **Haobo Dai:** Validation. **Yang Yang:** Supervision, Writing – review & editing. **Chenghang Zheng:** Conceptualization, Supervision, Writing – review & editing, Funding acquisition. **Xiang Gao:** Conceptualization, Supervision.

Declaration of Competing Interest

The authors declare that they have no known competing financial interests or personal relationships that could have appeared to influence the work reported in this paper.

Acknowledgement

This work is supported by Development Plan of Shandong Province of China (2020CXGC011401) and the National Natural Science Foundation of China (U1609212 and 52076191).

References

[1] D. Flagiello, A. Erto, A. Lancia, F. Di Natale, Experimental and modelling analysis of seawater scrubbers for sulphur dioxide removal from flue-gas, Fuel 214 (2018) 254–263, https://doi.org/10.1016/j.fuel.2017.10.098.
[2] J. Teuchies, T.J.S. Cox, K. Van Itterbeeck, F.J.R. Meysman, R. Blust, The impact of scrubber discharge on the water quality in estuaries and ports, Environ. Sci. Europe 32 (1) (2020) 103, https://doi.org/10.1186/s12302-020-00380-z.
[3] M.A. Churchill S, Brown P, Del Vento S, Karagianni E, Murrells T, Passant N, Richardson J, Richmond B, Smith H, Stewart R, Tsagatakis I, Thistlethwaite G, Wakeling D, Walker C, Wiltshire J, Hobson M, Gibbs M, Misselbrook T, Dragosits U, Tomlinson S, UK Informative Inventory Report (1990 to 2019) Ricardo Energy & Environment, Aether, Rothamsted Research, UKCEH, London, 2021.
[4] C.W. Hilda Huang, 2018 Hong Kong Emission Inventory Report, Air Science Group, Environmental Protection Department, The Government of the Hong Kong Special Administrative Region, Hongkong, China, 2020.
[5] J. Shen, C. Zheng, L. Xu, Y. Zhang, Y. Zhang, S. Liu, X. Gao, Atmospheric emission inventory of SO3 from coal-fired power plants in China in the period 2009–2014, Atmos. Environ. 197 (2019) 14–21, https://doi.org/10.1016/j.atmosenv.2018.10.008.
[6] H. Wang, B. Yuan, R. Hao, Y. Zhao, X. Wang, A critical review on the method of simultaneous removal of multi-air-pollutant in flue gas, Chem. Eng. J. 378 (2019) 122155, https://doi.org/10.1016/j.cej.2019.122155.
[7] C. Zheng, Y. Wang, Y. Liu, Z. Yang, R. Qu, D. Ye, C. Liang, S. Liu, X. Gao, Formation, transformation, measurement, and control of SO3 in coal-fired power plants, Fuel 241 (2019) 327–346, https://doi.org/10.1016/j.fuel.2018.12.039.
[8] I. Panasiuk, L. Turkina, The evaluation of investments efficiency of SOx scrubber installation, Trans. Res. Part D: Trans. Environ. 40 (2015) 87–96, https://doi.org/10.1016/j.trd.2015.08.004.
[9] C. Schembari, F. Cavalli, E. Cuccia, J. Hjorth, G. Calzolai, N. Pérez, J. Pey, P. Prati, F. Raes, Impact of a European directive on ship emissions on air quality in Mediterranean harbours, Atmos. Environ. 61 (2012) 661–669, https://doi.org/10.1016/j.atmosenv.2012.06.047.
[10] C. Wang, J.J. Corbett, J.J. Winebrake, Cost-effectiveness of reducing sulfur emissions from ships, Environ. Sci. Technol. 41 (24) (2007) 8233–8239, https://doi.org/10.1021/es070812w.
[11] J. Chen, Z. Wan, H. Zhang, X. Liu, Y. Zhu, A. Zheng, Governance of Shipping Emission of SOx in China's Coastal Waters: The SECA Policy, Challenges, and Directions, Coastal Management 46(3) (2018) 191-209. https://doi.org/10.1080/08920753.2018.1451727.
[12] J. Liu, O. Duru, A.-W.-K. Law, Assessment of atmospheric pollutant emissions with maritime energy strategies using bayesian simulations and time series forecasting, Environ. Pollut. 270 (2021) 116068, https://doi.org/10.1016/j.envpol.2020.116068.
[13] H. Winnes, E. Fridell, J. Moldanová, Effects of marine exhaust gas scrubbers on gas and particle emissions, J. Marine Sci. Eng. 8 (4) (2020) 299, https://doi.org/10.3390/jmse8040299.
[14] G. Caiazzo, G. Langella, F. Miccio, F. Scala, An experimental investigation on seawater SO2 scrubbing for marine application, Environ. Prog. Sustain. Energy 32 (4) (2013) 1179–1186, https://doi.org/10.1002/ep.11723.
[15] P. Olander, P. Hollman, S. Jacobson, Piston ring and cylinder liner wear aggravation caused by transition to greener ship transports–comparison of samples from test rig and field, Wear 302 (1) (2013) 1345–1350, https://doi.org/10.1016/j.wear.2012.12.028.
[16] D.W. Abel, T. Holloway, J. Martínez-Santos, M. Harkey, M. Tao, C. Kubes, S. Hayes, Air quality-related health benefits of energy efficiency in the United States, Environ. Sci. Technol. 53 (7) (2019) 3987–3998, https://doi.org/10.1021/acs.est.8b06417.
[17] V. Ciatteo, G. Giacchetta, B. Marchetti, Dynamic model for the economical evaluation of different technical solutions for reducing naval emissions, IJPQM 14 (3) (2014) 314, https://doi.org/10.1504/IJPQM.2014.064808.
[18] Y. Zhu, X. Tang, T. Li, Y. Ji, Q. Liu, L. Guo, J. Zhao, Shipboard trials of magnesium-based exhaust gas cleaning system, Ocean Eng. 128 (2016) 124–131, https://doi.org/10.1016/j.oceaneng.2016.10.004.
[19] Z.L. Yang, D. Zhang, O. Caglayan, I.D. Jenkinson, S. Bonsall, J. Wang, M. Huang, X. P. Yan, Selection of techniques for reducing shipping NOx and SOx emissions, Trans. Res. Part D: Trans. and Environ. 17 (6) (2012) 478–486, https://doi.org/10.1016/j.trd.2012.05.010.
[20] R. Huang, H. Wu, L. Yang, Study on the ammonia emission characteristics in an ammonia-based WFGD system, Chem. Eng. J. 379 (2020) 122257, https://doi.org/10.1016/j.cej.2019.122257.
[21] L.E. Kallinikos, E.I. Farsari, D.N. Spartinos, N.G. Papayannakos, Simulation of the operation of an industrial wet flue gas desulfurization system, Fuel Process. Technol. 91 (12) (2010) 1794–1802, https://doi.org/10.1016/j.fuproc.2010.07.020.
[22] C. Brogren, H.T. Karlsson, Modeling the absorption of SO2 in a spray scrubber using the penetration theory, Chem. Eng. Sci. 52 (18) (1997) 3085–3099, https://doi.org/10.1016/S0009-2509(97)00126-7.
[23] Y. Zhong, X. Gao, W. Huo, Z.-Y. Luo, M.-J. Ni, K.-F. Cen, A model for performance optimization of wet flue gas desulfurization systems of power plants, Fuel Process. Technol. 89 (11) (2008) 1025–1032, https://doi.org/10.1016/j.fuproc.2008.04.004.
[24] S. Darake, M.S. Hatamipour, A. Rahimi, P. Hamzeloui, SO2 removal by seawater in a spray tower: experimental study and mathematical modeling, Chem. Eng. Res. Des. 109 (2016) 180–189, https://doi.org/10.1016/j.cherd.2015.11.027.
[25] S. Darake, A. Rahimi, M.S. Hatamipour, P. Hamzeloui, SO2removal by seawater in a packed-bed tower: experimental study and mathematical modeling, Sep. Sci. Technol. 49 (7) (2014) 988–998, https://doi.org/10.1080/01496395.2013.872660.
[26] G. Caiazzo, A. Di Nardo, G. Langella, F. Scala, Seawater scrubbing desulfurization: a model for SO2 absorption in fall-down droplets, Environ. Prog. Sustainable Energy 31 (2) (2012) 277–287, https://doi.org/10.1002/ep.10541.
[27] X.J. Tang, T. Li, H. Yu, Y.M. Zhu, Prediction model for desulphurization efficiency of onboard magnesium-base seawater scrubber, Ocean Eng. 76 (2014) 98–104, https://doi.org/10.1016/j.oceaneng.2013.11.009.
[28] Q. Liu, Y. Zhu, X. Tang, T. Li, W. Liu, J. Zhao, Q. Li, Modeling and prediction of desulfurization efficiency for magnesium-based seawater exhaust gas clean system, Proceedings of the Institution of Mechanical Engineers, Part M: Journal of Engineering for the Maritime Environment 233(1) (2017) 325-332. https://doi.org/10.1177/1475090217744905.
[29] J.A. Michalski, Aerodynamic characteristics of flue gas desulfurization spray towerspolydispersity consideration, Ind. Eng. Chem. Res. 39 (9) (2000) 3314–3324, https://doi.org/10.1021/ie990791h.
[30] Z. Zhao, Y. Zhang, W. Gao, J. Baleta, C. Liu, W. Li, W. Weng, H. Dai, C. Zheng, X. Gao, Simulation of SO2 absorption and performance enhancement of wet flue gas desulfurization system, Process Saf. Environ. Prot. 150 (2021) 453–463, https://doi.org/10.1016/j.psep.2021.04.032.
[31] M. Gerbec, A. Stergaršek, R. Kocjančič, Simulation model of wet flue gas desulphurization plant, Comput. Chem. Eng. 19 (1995) 283–286, https://doi.org/10.1016/0098-1354(95)87050-4.
[32] E.N. Fuller, P.D. Schettler, J.C. Giddings, New method for prediction of binary gas-phase diffusion coefficients, Ind. Eng. Chem. 58 (5) (1966) 18–27, https://doi.org/10.1021/ie50677a007.
[33] W. Pasiuk-Bronikowska, K.J. Rudziński, Absorption of SO2 into aqueous systems, Chem. Eng. Sci. 46 (9) (1991) 2281–2291, https://doi.org/10.1016/0009-2509(91)85126-I.
[34] J.B. Angelo, E.N. Lightfoot, D.W. Howard, Generalization of the penetration theory for surface stretch: application to forming and oscillating drops, AIChE J. 12 (4) (1966) 751–760, https://doi.org/10.1002/aic.690120423.
[35] A. Olsen, R.M. Key, S. van Heuven, S.K. Lauvset, A. Velo, X. Lin, C. Schirnick, A. Kozyr, T. Tanhua, M. Hoppema, S. Jutterström, R. Steinfeldt, E. Jeansson, M. Ishii, F.F. Pérez, T. Suzuki, The global ocean data analysis project version 2 (GLODAPv2) – an internally consistent data product for the world ocean, Earth Syst. Sci. Data 8 (2) (2016) 297–323, https://doi.org/10.5194/essd-8-297-2016.
[36] S.K. Lauvset, R.M. Key, A. Olsen, S. van Heuven, A. Velo, X. Lin, C. Schirnick, A. Kozyr, T. Tanhua, M. Hoppema, S. Jutterström, R. Steinfeldt, E. Jeansson, M. Ishii, F.F. Perez, T. Suzuki, S. Watelet, A new global interior ocean mapped climatology: the 1° × 1° GLODAP version 2, Earth Syst. Sci. Data 8 (2) (2016) 325–340, https://doi.org/10.5194/essd-8-325-2016.
[37] R.M. Key, A. Olsen, S. van Heuven, S. K. Lauvset, A. Velo, X. Lin, C. Schirnick, A. Kozyr, T. Tanhua, M. Hoppema, S. Jutterström, R. Steinfeldt, E. Jeansson, M. Ishi, F. F. Perez, T. Suzuki., Global Ocean Data Analysis Project, Version 2 (GLODAPv2), Carbon Dioxide Information Analysis Center, Oak Ridge National Laboratory, US Department of Energy, Oak Ridge, Tennessee., 2015.